the possibility of obtaining the same complexes starting from other Fe materials such as α-Fe_2O_3, $FeCl_3$, and hydrated $Fe_2(SO_4)_3$. Following the same procedure as the one described for the synthesis of the α-phase in acetone, $FeCl_3$ (homogeneous medium) and hydrated $Fe_2(SO_4)_3$ (heterogeneous medium) led to the α-phase in 40% and 80% yield, respectively. No reaction was observed starting from α-Fe_2O_3. The conclusion is that the layered nature of FeOCl is not actually necessary for this synthesis. Nevertheless this study is a contribution to the identification and the preparation of new ironphosphonates.

Work is currently in progress to extend the synthetic chemistry of derivatized layered ironphosphonates via FeOCl, by studying the effects of the substituents borne by various phosphonic acids (R = alkyl, carboxylic acids, alcohol, etc.) and the possibility of making specific organic reactions in their interlayer space, especially when functional organic groups are bound to phosphorus.

Acknowledgment. We acknowledge the Commission of European Communities for support of this work under Grant No. MA1E-0030-C.

Registry No. I, 128752-87-4; II, 72702-16-0; FeOCl, 13870-10-5; $FeCl_3$, 7705-08-0; $Fe_2(SO_4)_3$, 10028-22-5.

Supplementary Material Available: Tables of anisotropic thermal parameters, positional parameters for hydrogen atoms, and a complete list of bond lengths and angles (3 pages); final observed and calculated structure factors (4 pages). Ordering information is given on any current masthead page.

Growth and Characterization of Gallium Arsenide Using Single-Source Precursors: OMCVD and Bulk Pyrolysis Studies

James E. Miller,[1a] Kenneth B. Kidd,[1b] Alan H. Cowley,*[,1b] Richard A. Jones,*[,1b] John G. Ekerdt,[1a] Henry J. Gysling,*[,1c] Alex A. Wernberg,[1c] and Thomas N. Blanton[1d]

Departments of Chemical Engineering and Chemistry, The University of Texas at Austin, Austin, Texas 78712, and Corporate Research Laboratories and Analytical Technology Division, Eastman Kodak Company, Rochester, New York 14650

Received March 12, 1990

Films of gallium arsenide have been grown on GaAs(100), GaAs(111), and α-Al_2O_3(0001) at 1×10^{-4} Torr and 525 °C by using a single-source precursor $[Me_2Ga(\mu\text{-}t\text{-}Bu_2As)]_2$ (1) and H_2 carrier gas. These conditions resulted in GaAs growth rates of 0.75 μm/h. The carbon content of the films was less than the XPS detection limit (1000 ppm). Secondary ion mass spectrometry (SIMS) revealed that carbon was not incorporated from the precursor. Photoluminescence spectra (5 K) of the material grown on α-Al_2O_3(0001) exhibited the 1.52-eV bandgap of GaAs. However, the material appears degeneratively doped. X-ray diffraction, Berg–Barrett topography, and pole figure analysis indicated that these GaAs films are (111) orientated and polycrystalline. Mass spectroscopic analysis of the OMCVD reaction of 1 revealed that the volatile products are predominantly isobutylene and methane. Bulk pyrolysis studies demonstrated that at lower temperatures (350 °C) the decomposition of 1 is incomplete and that isobutane is produced in addition to isobutylene and methane. Under similar conditions, the decomposition of $[n\text{-}Bu_2Ga(\mu\text{-}t\text{-}Bu_2As)]_2$ (2) is virtually complete. The thermolysis of 2 produced isobutane (60%), isobutylene (32%), *n*-butane (9.6%), 1-butene (44%), *trans*-2-butene (26%), and *cis*-2-butene (19%).

Introduction

Organometallic chemical vapor deposition (OMCVD) has become a leading technique for producing epitaxial films of group III–V compound semiconductors. Typically, OMCVD processes employ a group III trialkyl such as Me_3Ga and a group V hydride such as AsH_3. Reaction of the group III and V sources in the temperature range 600–700 °C results in the desired semiconducting films.[2] However, despite its widespread use the conventional OMCVD method suffers from a number of drawbacks. The high toxicity of AsH_3 and the pyrophoric nature of the group III alkyls represent health, safety, and environmental hazards.[2-8] Other problems that have been encountered include carbon contamination and prereactions, particularly in the case of InP growth. Furthermore, it is desirable to lower the deposition temperatures to minimize the interdiffusion of layers and dopants. Various attempts have been made to address these problems. For example, modifications to the conventional OMCVD have been developed, and the use of alternative group V and to a lesser extent group III sources have been investigated.[9-18] An interesting alternative approach has been to

(1) (a) Department of Chemical Engineering, UT Austin. (b) Department of Chemistry, UT Austin. (c) Corporate Research Laboratories, Eastman Kodak Company. (d) Analytical Technology Division, Eastman Kodak Company.

(2) Ludowise, M. J. *J. Appl. Phys.* **1985**, *58*, R31.
(3) Lum, R. M.; Klingert, J. K.; Dutt, B. V. *J. Cryst. Growth* **1986**, *75*, 421.
(4) Shastry, S. K.; Zemon, S.; Kenneson, D. G.; Lambert, G. *Appl. Phys. Lett.* **1988**, *52*, 150.
(5) Kuech, T. F.; Veuhoff, E. *J. Cryst. Growth* **1984**, *68*, 148.
(6) Stringfellow, G. B. *J. Cryst. Growth* **1986**, *75*, 91.
(7) Bradley, D. C.; Faktor, M. M.; Scott, M.; White, E. A. D. *J. Cryst. Growth* **1986**, *75*, 101.
(8) Moss, R. H. *J. Cryst. Growth* **1984**, *68*, 78.
(9) Larsen, C. A.; Chen, C. H.; Kitamura, M.; Stringfellow, G. B.; Brown, D. W.; Robertson, A. J. *Appl. Phys. Lett.* **1986**, *48*, 1531.
(10) Kurtz, S. R.; Olson, J. M.; Kibbler, A. *J. Electron. Mater.* **1989**, *18*, 15.
(11) Kellert, F. G.; Whelan, J. S.; Chan, K. T. *J. Electron. Mater.* **1989**, *18*, 355.

0897-4756/90/2802-0589$02.50/0

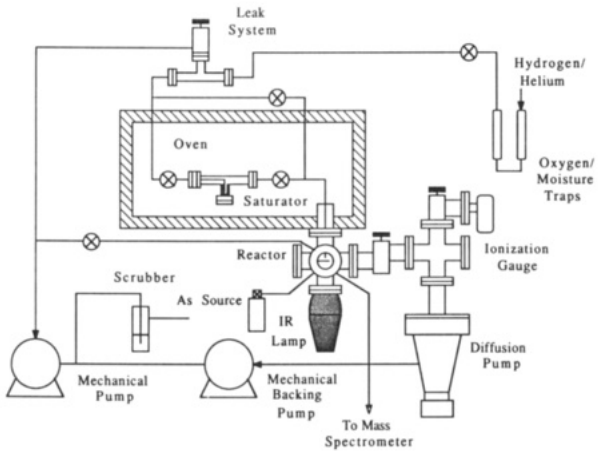

Figure 1. Reactor system schematic.

use adducts such as $Me_3In{\cdot}PEt_3$ as film precursors.[8,19-25] Such adducts are less reactive than the separate components and are therefore easier to purify and handle. However, although most adducts feature the desired 1:1 stoichiometry for the group III and V elements, the donor–acceptor bonds are generally weak and thus prone to rupture prior to or during film growth. Typically the resulting loss of stoichiometry is addressed by employing an excess of PH_3 or AsH_3.[20,21,25]

Recently, we have developed single-source precursors for the production of group III–V compound semiconductors.[26] These precursors are of the general type $(L_nMEL'_n)_x$, where M and E are group III and V elements, respectively, and L_n and L'_n are ligands that are capable of facile thermal decomposition. A basic design feature of the precursors is that the M–E bonds are of the two-center two-electron type and thus stronger than the donor–acceptor linkages of adducts. It was our intention that the M–E bonds would remain intact during the ligand decomposition processes. In the present paper we report the details of OMCVD studies of the deposition of GaAs from the single-source precursor $[Me_2Ga\text{-}\mu\text{-}t\text{-}Bu_2As]_2$ (1). The resulting films have been characterized by a variety of techniques including X-ray photoelectron spectroscopy (XPS), secondary ion mass spectrometry (SIMS), photoluminescence spectroscopy (PL), X-ray diffraction (XRD), Berg–Barrett topography, and pole figure analysis. Lower temperature bulk pyrolysis studies of 1 and $[n\text{-}Bu_2Ga\text{-}\mu\text{-}t\text{-}Bu_2As]_2$ (2) have also been carried out. The volatile products from OMCVD reactions of 1 and the bulk pyrolysis studies have been characterized by mass spectroscopy.

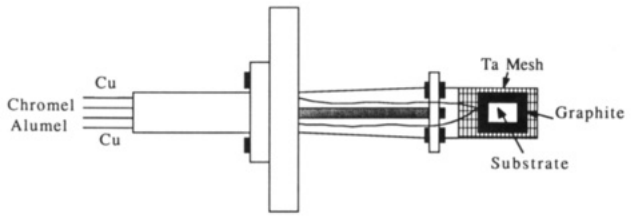

Figure 2. Schematic of the stage assembly.

Experimental Section

Gas-Phase OMCVD Studies. A schematic view of the OMCVD cold-wall reactor is presented in Figure 1. The reactor featured a six-way stainless steel vacuum cross (tube o.d. 3.8 cm). The cross was roughed with a mechanical pump or evacuated with an oil diffusion pump (pumping speed 322 L/s). The precursor 1 was dosed vertically through a 0.9-cm Pyrex tube onto 1 × 1 cm substrates. The exit of the doser was placed 0.5 cm above the surface of the substrate. A 0.32-cm stainless steel tube permitted the introduction of a second compound. Figure 2 provides details of the sample stage assembly. The horizontally arranged substrates rested on a SiC-coated graphite susceptor that was supported by Ta mesh. Heating (up to 750 °C) was provided by an IR beam focused on the susceptor underside. If necessary, supplementary heating could be generated by passing an electric current through the Ta mesh. Feedthroughs allowed temperature determination by means of a thermocouple that was spot welded onto the mesh. The reactor walls were cooled by flowing air over them and the reactor atmosphere was analyzed by an online, differentially pumped UTI Model 100C quadrupole mass spectrometer.

Compound 1 was loaded via drybox into a quartz thimble situated in a stainless steel saturator. The saturator comprised a high-vacuum tee (tube o.d. 1.9 cm) fitted with two high-temperature vacuum valves and a blank flange. The mass transport properties of the saturator were improved by directing the carrier gas via a 0.32-cm stainless tube onto the leg of the tee that contained 1. The hydrogen carrier gas was fed to the saturator through a leak valve, and the reactor pressure was controlled by adjustment of the carrier gas-flow rate. The temperature of the saturator was maintained at 145 °C by an oven, and the saturator outlet was connected directly to the Pyrex doser.

The following substrates were used in the present study: α-Al_2O_3(0001), GaAs(100), and GaAs(111). The α-Al_2O_3 substrates were degreased in tetrachloroethylene, followed by sequential rinses in MeOH and DI water prior to being blown dry and loaded into the reactor. A similar protocol was employed for the GaAs substrates; however, they were etched in an 8:1:1 solution of H_2SO_4:H_2O_2:H_2O and then rinsed in DI water prior to loading into the reactor. When the substrates were in place, the reactor pressure was reduced to 1×10^{-6} Torr and the oven containing the saturator was brought to 145 °C. The α-Al_2O_3 substrates were then brought to reaction temperature by turning on the IR lamp. The saturator containing 1 was opened to the reactor, and the carrier gas flow was adjusted to give a reactor pressure of 1×10^{-4} Torr.

XPS data were obtained on a VG Scientific ESCALAB Mark II instrument with a Mg Kα X-ray anode. A Leybold Heraus LHS-2 surface analysis system was used to collect the SIMS data. The samples were sputtered with a 3–4-μA Ar^+ ion beam until the O^+ signal (mass 16) disappeared prior to collecting the SIMS spectra. Care was also taken that the grown GaAs layer was not removed.

X-ray Diffraction. Phase identification and in-plane orientation measurements were made using a Rigaku RU-300 Bragg–Brentano diffractometer with copper radiation, diffracted beam

(12) Li, S. H.; Larsen, C. A.; Buchan, N. I.; Stringfellow, G. B. *J. Electron. Mater.* **1989**, *18*, 457.
(13) Lum, R. M.; Klingert, J. K.; Lamont, M. G. *Appl. Phys. Lett.* **1987**, *50*, 284.
(14) Chen, C. H.; Cao, D. S.; Stringfellow, G. B. *J. Electron. Mater.* **1988**, *17*, 67.
(15) Larsen, C. A.; Buchan, N. I.; Li, S. H.; Stringfellow, G. B. *J. Cryst. Growth* **1989**, *94*, 663.
(16) Larsen, C. A.; Li, S. H.; Buchan, N. I.; Stringfellow, G. B. *J. Cryst. Growth* **1989**, *94*, 673.
(17) Chen, C. H.; Larsen, C. A.; Stringfellow, G. B. *Appl. Phys. Lett.* **1987**, *50*, 218.
(18) Lum, R. M.; Klingert, J. K.; Wynn, A. S.; Lamont, M. G. *Appl. Phys. Lett.* **1988**, *52*, 1475.
(19) Bradley, D. C.; Faktor, M. M.; White, E. A. D.; Frigo, D. M.; Young, K. V. *Chemtronics* **1988**, *3*, 50.
(20) Bass, S. J.; Skolnick, M. S.; Chudzynska, H.; Smith, L. *J. Cryst. Growth* **1986**, *75*, 221.
(21) Zaouk, A.; Salvetat, E.; Sakaya, J.; Maury, F.; Constant, G. *J. Cryst. Growth*, **1981**, *55*, 135.
(22) Maury, F.; El Hammadi, A.; Constant, G. *J. Cryst. Growth* **1984**, *68*, 88.
(23) Maury, F.; Constant, G.; Fontaine, P.; Biberian, J. P. *J. Cryst. Growth* **1986**, *78*, 185.
(24) Chatterjee, A. K.; Faktor, M. M.; Moss, R. H.; White, E. A. D. *J. Phys. (Paris)* **1982**, *C5*, 491.
(25) Haigh, J.; O'Brien, S. *J. Cryst. Growth* **1984**, *68*, 550.
(26) For a preliminary communication, see: Cowley, A. H.; Benac, B. L.; Ekerdt, J. G.; Jones, R. A.; Kidd, K. B.; Lee, J. Y.; Miller, J. E. *J. Am. Chem. Soc.* **1988**, *110*, 6248.
(27) Sangster, R. D. In *Compound Semiconductors*; Willardson, R. K., Goering, H. L., Eds.; Reinhold: New York, 1962; Vol. 1.

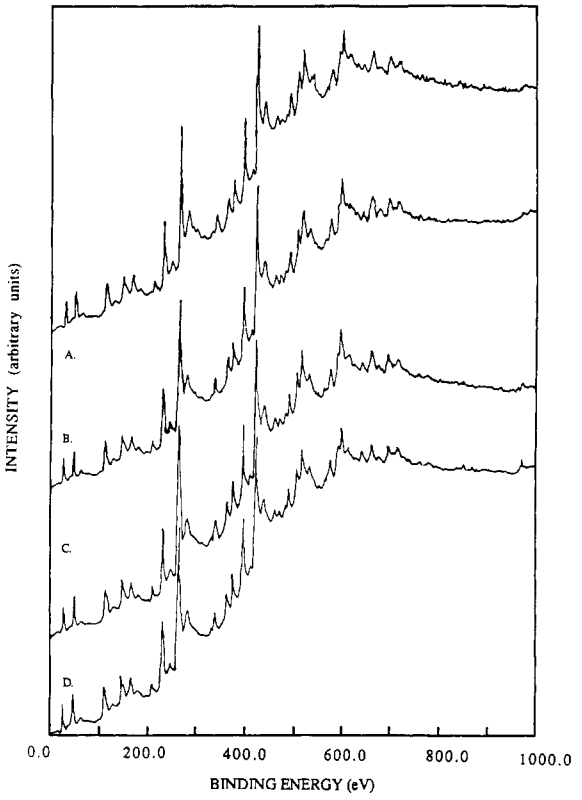

Figure 3. XPS spectra of (A) a GaAs(100) substrate, and films grown from 1 at (B) 700 °C in He, (C) 700 °C in H_2, and (D) 570 °C in H_2.

monochromator tuned for Cu Kα radiation, and a scintillation detector.

Pole figure analyses for quantitative orientation determinations were made in the reflection mode with a Rigaku Schultz type pole figure goniometer, copper radiation, diffracted beam nickel filter, and a scintillation detector. The pole figure data were corrected for background, absorption, and sample defocusing before normalizing the data. The random sample used for the sample defocusing correction was a pellet of gallium arsenide powder in an epoxy binder.

Berg–Barrett reflection topography was used to look for the presence of lattice defects. The Berg–Barrett system consists of a copper X-ray tube, 24-in. beam collimator, and a four-circle goniometer. For fast detection of the Cu Kα diffraction lines, a real-time detection system was used consisting of a Brimrose image intensifier tube, Hitachi CCD camera, Compaq 386 computer, and a Panasonic color monitor. For a final higher resolution image, Kodak SO-163 electron microscopy film and Kodak type 1A high-resolution plates were used for image capture.

Solid-State Bulk Pyrolysis Studies. Two types of experiment were carried out: (i) sealed tube pyrolyses to analyze the volatile products, and (ii) preparative scale pyrolyses to analyze the residual materials.

For the sealed tube pyrolyses, 5–20-mg samples of 1 or 2 were weighed into 10-mL head-space analysis vials inside a drybox, and the vials were sealed by using a Teflon-faced septum and an aluminum crimp seal. After removal of the sample from the drybox, the samples were placed on a heated aluminum receptacle maintained at 350 °C. The samples were covered with insulation up to the septum to minimize the condensation of gases on the walls of the vials. After 30 min, the headspace of the reaction vial was sampled and analyzed by injection into a gas chromatograph. An immediate transfer via hot syringe was used when sampling higher molecular weight components. More volatile components were sampled after the receptacles had cooled to room temperature. Gas chromatographic analyses were carried out on a Hewlett-Packard 5890A instrument. A Chromopack PLOT fused silica column with Al_2O_3 and KCl coating (50 m × 0.32 mm i.d.) was used for the more volatile components. A 15 m × 0.32 mm i.d. J and W DB 5 column containing 5% phenyl–95% silicone

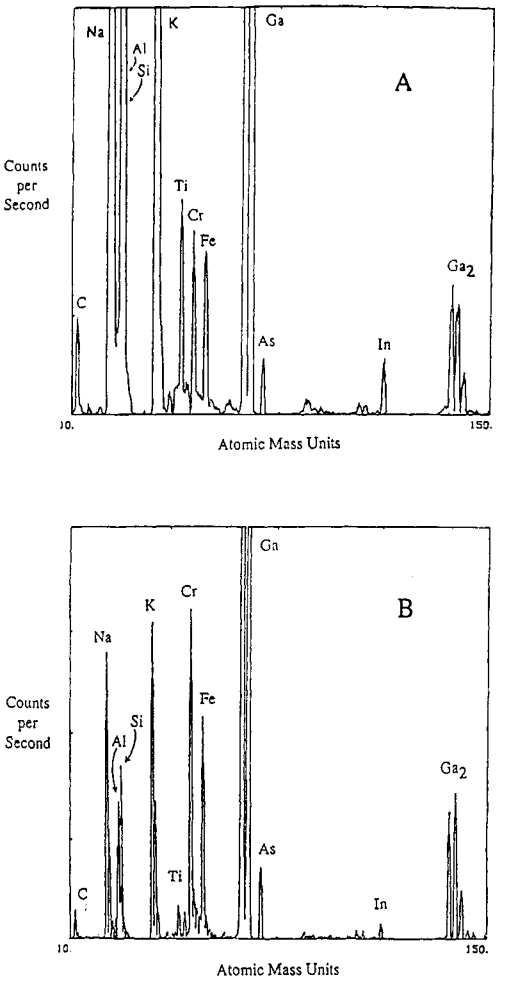

Figure 4. SIMS of (A) a GaAs(100) substrate at 0.25 μA and 5 keV and (B) a film grown from 1 (0.29 μA and 5 keV) on the GaAs substrate at 570 °C in H_2.

bonded film (0.32-μm thickness) was employed for the higher molecular weight components.

Preparative-scale pyrolyses were carried out in a Fisher Model 495 programmable ashing furnace. Samples were placed in a quartz reaction tube through which Ar was passed (100 mL/min) by using a mass flow controller. The following heating profiles were used: 1, 5 °C min^{-1} to 250 °C/hold 30 min/5 °C min^{-1} to 260 °C/hold 5 h; 2, 5 °C min^{-1} to 300 °C/hold 10 min/5 °C min^{-1} to 350 °C/hold 5 h. In the case of 1 the residue was annealed by heating for 5 h at 350 °C and 1 h at 500 °C.

X-ray diffraction patterns of the pyrolysis residues were recorded on a Philips PW 1840 X-ray diffractometer. Mass spectra were recorded on a MAT 731 field desorption mass spectrometer. The Raman system used for these studies consisted of a Spex 1403 double monochromator interfaced to a Spex Datamate dedicated microcomputer. The detector was a high-sensitivity GaAs photocathode RCA C31034 photomultiplier tube cooled thermoelectrically to approximately −25 °C.

Results and Discussion

OMCVD Studies. Initial experimentation focused on identifying the optimum conditions for delivery of the precursor 1 to the reactor. The best results were obtained when a reactor pressure of 1×10^{-4} Torr was employed. At lower pressures, radiative heat losses led to condensation of 1 in the doser. The use of higher pressures caused prereactions to occur in the doser. Either H_2 or He could be used as the carrier gas. The optimum saturator and reactor temperatures were found to be 145 and 525 °C, respectively. The use of higher reactor temperatures often resulted in deposits with a milky appearance, while lower temperatures caused slower growth rates. Use of the

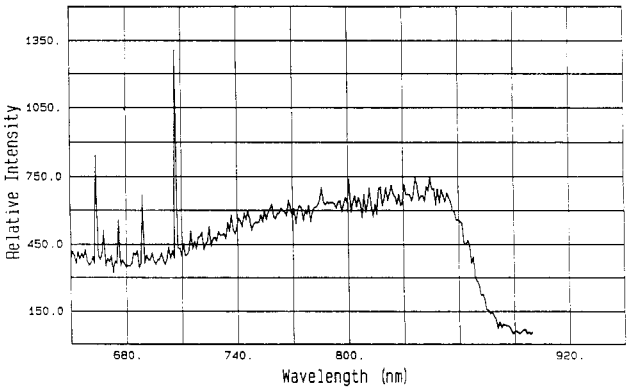

Figure 5. The 5 K photoluminescence spectrum of a GaAs film grown from 1 at 550 °C in H_2 on α-Al_2O_3(0001).

foregoing conditions resulted in growth rates of 0.75 μm/h as determined by profilometry.

The XPS of the GaAs films (Figure 3) are virtually indistinguishable from those of the GaAs substrate. Moreover, within experimental error the Ga:As mole ratio is 1:1, and no carbon peaks are detectable, thus implying that the carbon content is less than 1000 ppm. The SIMS spectra for both the silicon-doped GaAs substrate and a film grown from 1 show the presence of the metallic impurities Na, K, Al, Si, In, Ti, Cr, and Fe as well as carbon (Figure 4). The origin of the metallic impurities was not studied. It should be noted that these preliminary uncalibrated SIMS studies were performed only as an initial qualitative gauge of carbon incorporation. We plan further studies using internal standards to fully evaluate the levels of impurities. Examination of the carbon and As mass peak intensities reveals that, at the very least, no more carbon was present in films grown from 1 than was present in the substrate. Photoluminescence spectra (5 K) of the GaAs films deposited on α-Al_2O_3 exhibit an unusually broad band edge luminescence peak (Figure 5). At present we do not have a simple explanation for this, although it is likely caused by impurities and the polycrystalline structure (see below). The data were observed uniformly on scanning the laser beam across the GaAs layer.

Initial X-ray diffraction studies of the GaAs films deposited on α-Al_2O_3(0001) and GaAs(100) revealed diffraction patterns very similar to that of a GaAs(111) wafer. However, the samples on α-Al_2O_3(0001) exhibited some line broadening suggestive of strain and/or crystallite size effects. Berg–Barrett topographs of the films grown on GaAs(100) indicated that there was little stress on the surface of the wafer due to the presence of the thin film. Pole figure analysis was also implemented to investigate sample orientation and orientation distribution. The pole figure for a GaAs(111) wafer shows a single-crystal texture with (111) density in the pole figure center and at 70.5° tilt from the center (Figure 6A). The pole figure for the GaAs film on α-Al_2O_3(0001) exhibits heavy pole density both at the center and at 70.5° tilt away from the center (Figure 6B). However, the presence of a "ring" of poles at the 70.5° tilt angle indicates that the sample contains grains oriented with cylindrical symmetry along the normal to the sample plane much like a fiber texture. The GaAs film is thus highly (111) orientated in the sample plane but is polygrained with the grains cylindrically aligned along the normal to the sample plane. Similar results were obtained with the GaAs film deposited on GaAs(100). Interestingly, similar results have been obtained by Maury et al.[22] using the adduct $Me_2(C_6F_5)Ga{\cdot}AsEt_3$ as the GaAs source. In this case epitaxial growth was achieved on GaAs(111) substrates; however, with our compounds it was possible to grow only polycrystalline GaAs layers on GaAs(100), GaAs(111), and Ge(100). For typical GaAs deposition processes with separate Ga and As sources, growth in the (111) direction is inherently more difficult than in the (100) direction. One explanation is that our precursor presents groups of atoms to the surface with some of the GaAs bonds already formed. The (111) directions may result because this group of atoms is oriented with respect to the surface. However, since we are currently unable to characterize the substrates in situ prior to growth, we cannot rule out the possibility of surface contamination as a cause of the polycrystalline morphology. It is hoped that further insights will be provided by experiments, currently in progress, that employ static SIMS to detect reactive fragments on the growth surfaces.

On-line mass spectrometric analysis of the OMCVD reaction of 1 revealed that the volatile products are predominantly isobutylene, isobutane, and methane. A mechanism that will accommodate the formation of isobutylene and methane is

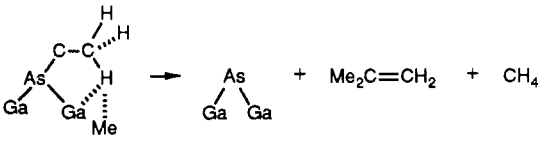

The salient feature is the interaction of Ga with a C–H

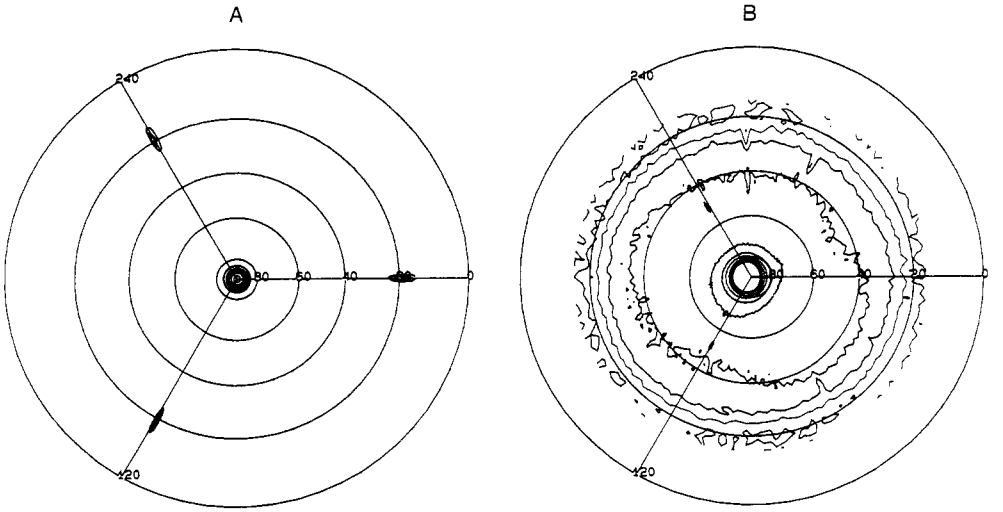

Figure 6. (A) Pole figure plot for a GaAs(III) (111) wafer. (B) Pole figure plot for a GaAs film grown from 1 at 550 °C in H_2 on α-Al_2O_3(0001).

bond of a *t*-Bu substituent. Such a β-hydride mechanism is consistent with the solid-state structure of **1**.[28] Although the H atoms were not located, placement of these atoms in idealized positions resulted in a "close" nonbonded distance of 2.62 Å. The formation of isobutane, however, implies the homolysis of the As–C bonds to form *tert*-butyl radicals followed by hydrogen abstraction from unreacted precursors. Clearly, labeling experiments will be needed to validate the above suggestions.

Solid-State Pyrolysis Studies. To analyze both the solid and volatile products from the pyrolysis experiments, two different sets of experimental conditions were employed. For the quantitative analysis of the volatile products a sample was heated to 350 °C in a closed reaction vial. The volatiles were then analyzed by GC/MS. To analyze the solids produced (i.e., GaAs) the samples of **1** were heated in an Ar flow in an oven with the temperature being programmed from ambient to 250 °C at 5 °C/min. The two techniques resulted in slight differences in the purity of the products. The residues from the closed-system experiments generally containing higher concentrations of organic residues than found for the flow system preparative pyrolysis. Despite these differences essentially the same conclusions may be drawn from the results of both experiments.

The preparative scale thermolysis of **1** at 260 °C in an Ar flow for 5 h gave a black residue that was shown to be amorphous by X-ray diffraction. However, the pyrolysis of **1** was incomplete, and a TGA scan of the residues indicated further weight loss that started at approximately 400 °C. Further heating of the residue for 5 h at 350 °C and an additional 1 h at 500 °C resulted in the formation of polycrystalline GaAs as shown by Raman and X-ray diffraction measurements.[29] The GaAs particle series as calculated from the diffraction peak widths were as follows: 260 °C, <25 Å; 350 °C, 30 Å; 500 °C, 60 Å. They may be compared to particle sizes of >1000 Å for the ground wafer. Consistent with the observation that the pyrolysis of **1** is incomplete at 260 °C in the sealed system, only approximately 50% of the theoretical quantity of hydrocarbons was evolved. Elemental analysis of the residue indicated C = 10% and H = 2.4%. Analysis of the volatiles produced indicated the presence of isobutane (21.4%), isobutylene (28.4%), and methane (50.0%). From these data under solid-state pyrolysis conditions, it appears that the first two methyl groups of **1** are eliminated at lower temperatures while the second two methyl groups are eliminated only at higher temperatures. As noted for the OMCVD studies, labeling studies currently in progress will hopefully clarify the suggested mechanistic pathways involved.

Interestingly, the total quantity of hydrocarbons evolved in the sealed-tube pyrolysis of **2** under conditions similar to those for **1** was quantitative within experimental error (±5%) and suggest that the thermal decomposition of the *n*-butyl-substituted precursor (**2**) is much more facile than that for the corresponding methyl analogue (**1**). The liberated hydrocarbons were isobutylene (32%), isobutane (60%), *n*-butane (9.6%), and *n*-butenes (82%), and the molar quantities of hydrocarbons liberated from the *tert*-butyl groups were equal to those attributable to the *n*-butyl groups. The use of longer reaction times and higher temperatures resulted in the formation of *cis*- and *trans*-2-butenes. The pyrolysis residue after heating to 350 °C for 5 h was shown to be polycrystalline GaAs by Raman spectroscopy and X-ray diffraction. However, elemental analysis revealed a small carbon content (1.6%). The formation of 1-butene and isobutane in the case of **2** can be explained by the following β-hydrogen transfer involving an *n*-Bu group:

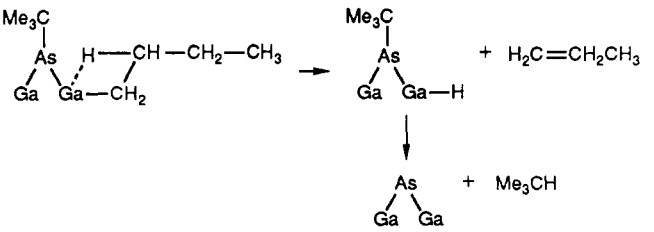

A competing mechanism, analogous to that proposed for **1**, would be responsible for the formation of isobutylene and *n*-butane. Finally, it is possible that the 2-butenes are formed by a metal-catalyzed isomerization of the 1-butene since the former were produced at the expense of the latter.

Conclusions

As shown by the initial materials characterization studies, the quality of the GaAs grown by OMCVD in this work is inadequate for device work. Several explanations may account for the poor film quality. Our apparatus does not allow us to characterize the substrate surfaces in situ before film growth. However, the use of our oil-based diffusion pump probably leads to sufficient surface contamination to prevent epitaxial growth. Future studies will be aimed at achieving epitaxial growth. We clearly require more stringent growth conditions in which the levels of oxygen and moisture in the system are reduced and a system in which the substrates can be characterized in situ. An apparatus specifically designed for this purpose is currently under construction.

Acknowledgment. We are grateful to the Army Research Office, the National Science Foundation, and the Robert A. Welch Foundation for financial support. R.A.J. thanks the Alfred P. Sloan foundation for a fellowship (1985–89). T.N.B. thanks Mark Morse for collection of Berg–Barrett data.

Registry No. 1, 106417-80-5; 2, 106417-81-6; gallium arsenide, 1303-00-0.

(28) Arif, A. M.; Benac, B. L.; Cowley, A. H.; Geerts, R. L.; Jones, R. A.; Kidd, K. B.; Power, J. M.; Schwab, S. T. *J. Chem. Soc., Chem. Commun.* **1986**, 1543.

(29) GaAs particle sizes were calculated from the diffraction peak widths by using the equation $B = (0.9\,\lambda/\cos\theta)$, where B = width of XRD peak at half-maximum in radians, $1° = (\pi/180)$ rad, λ = wavelength of X-radiation (1.5418 Å for Cu Kα), t = particle diameter in Å, and 2θ = peak maximum.